Capillary filling of nematic liquid crystals

Xiang-Dong Mi and Deng-Ke Yang*
Chemical Physics Interdisciplinary Program, Liquid Crystal Institute, Kent State University, Kent, Ohio 44242
(Received 20 March 1998)

We studied the orientation of nematic liquid crystals when they were being filled into cells by capillary action. We found that, in the flow front, the liquid crystal was always aligned along the flow direction. Far behind the flow front, the orientation of the liquid crystal depended on the anchoring direction of the alignment layers and the direction and speed of the flow. In cells with the anchoring direction parallel to the flow direction, the liquid crystal always oriented along the flow direction. In cells with the anchoring direction perpendicular to the flow direction, at low flow speed gradients, the liquid crystal orientated uniformly along the anchoring direction; at high flow speed gradients, the liquid crystal in bulk was tilted to the flow direction. The experimentally observed critical flow speed gradient was in agreement with the theoretical prediction. [S1063-651X(98)02608-7]

PACS number(s): 42.70.Df, 61.30.−v, 64.70.Md

INTRODUCTION

Liquid crystal displays, such as the twisted nematic display and the ferroelectric liquid crystal display, usually have alignment layers coated on their inner surfaces [1]. At static state, liquid crystals orient along the anchoring direction of the alignment layers. In the fabrication of liquid crystal displays, liquid crystals are filled into the display cells by capillary action or forced into the cells by pressure. In the filling process, the orientation of the liquid crystal is determined by its velocity, viscosity coefficients, and the alignment layers. In some circumstances, the liquid crystal is not uniformly aligned along the anchoring direction of the alignment layer, and exerts a torque on the molecules of the alignment layer and may damage the alignment layer. It is important to understand the orientation of liquid crystals when they are being filled into display cells.

The orientation of liquid crystals in motion is very interesting and complicated because of the coupling between the liquid crystal director and the velocity field [2,3]. A flow of a nematic liquid crystal sometimes causes it to reorient in order to reduce the entropy production [4,5]. A reorientation of the liquid crystal sometimes causes it to flow (called backflow) [6].

There are many works done on the hydrodynamics of nematic liquid crystals. Most of them were performed in thick cells ($\geqslant 100\ \mu$m) and under external fields. We studied the flow alignment of nematic liquid crystals when they were being filled into thin cells ($\leqslant 50\ \mu$m) by capillary action as in fabrication of liquid crystal displays. We organize this paper in the following way. First, we present our theoretical study on the alignment of nematic liquid crystals in capillary filling. Then we report the results of our experimental study.

THEORETICAL STUDY

Flow speed in capillary filling

We consider the flow of a nematic liquid crystal in a rectangular cell consisting of two long parallel plates. The cell has an alignment layer on the inner surface of the two plates. The geometry of the flow of the liquid crystal and the axes of the coordinate are shown in Fig. 1. On the surface of the cell, the liquid crystal is anchored either along the x direction or along the y direction by the alignment layer. The motion of the liquid crystal in the flow front is very complicated. Here we consider the motion of the liquid crystal far behind the flow front. The velocity of the liquid crystal is in the y direction and its value depends only on z, which is perpendicular to the plates. It is described by

$$\vec{V}=[0,u(z),0]. \tag{1}$$

If the orientation of the liquid crystal is uniform, then for a steady flow, the equation of motion (Navier-Stokes equation) is

$$\frac{\partial^2 u}{\partial z^2}=\frac{1}{\eta}\nabla P, \tag{2}$$

where ∇P is the pressure gradient and η is the translational viscosity coefficient, which is dependent on the orientation of the liquid crystal [2]. When the liquid crystal is along the y direction at any z plane, the viscosity coefficient is η_2; when the liquid crystal is along the x direction at any z

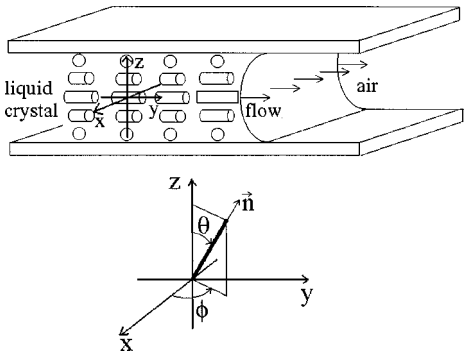

FIG. 1. Schematic diagram of the flow and orientation of the liquid crystal in the capillary filling.

*Author to whom correspondence should be addressed. Electronic address: dyang@kentvm.kent.edu

plane, the viscosity coefficient is η_3 (which is larger than η_2). If the pressure gradient is a constant, the solution of Eq. (2) is found to be parabolic:

$$u=\frac{-\nabla P}{2\eta}\left(\frac{d^2}{4}-z^2\right). \tag{3}$$

The flow speed at the middle layer ($z=0$) is

$$V=\frac{-\nabla P d^2}{8\eta}. \tag{4}$$

The averaged speed is

$$\overline{u}=\frac{\int_{-d/2}^{d/2}u\,dz}{d}=\frac{-\nabla P}{12\eta}\,d^2=\frac{2}{3}\,V. \tag{5}$$

The front of the liquid crystal flow moves at the averaged speed. In capillary filling, the front of the liquid crystal is curved because of the surface tension between the liquid crystal and the alignment layer on the plates. The curved surface at the front creates the pressure gradient throughout the liquid crystal [7]. The pressure gradient is found to be

$$\nabla P=\frac{-2(\gamma_{sv}-\gamma_{sl})}{ld}, \tag{6}$$

where l is the length of the liquid crystal inside the cell, γ_{sv} is the surface tension between the alignment layer and the air, and γ_{sl} is the surface tension between the alignment layer and the liquid crystal. The speed of the liquid crystal flow front is

$$\overline{u}=\frac{(\gamma_{sv}-\gamma_{sl})}{6\eta l}\,d. \tag{7}$$

$\Delta\gamma=\gamma_{sv}-\gamma_{sl}$ can be measured by the capillary rise method. For a vertical cylindrical capillary tube with the bottom of the tube in the liquid crystal, the height of the rise of the liquid crystal is given by

$$h=\frac{2(\gamma_{sv}-\gamma_{sl})}{Rg\rho}, \tag{8}$$

where R is the radius of the tube, ρ is the mass density of the liquid crystal, and g is the gravity constant.

Flow-induced Freedericksz transition in capillary filling

The translational motion and rotational motion of the liquid crystal are coupled. When the flow speed gradient of the liquid crystal is large enough, the translational motion of the liquid crystal will cause the liquid crystal director to rotate. In capillary filling, the liquid crystal molecules in the bulk flow but not the molecules on the surfaces; there is a speed gradient that may induce an orientational transition. Some theoretical studies have been performed on this problem and the reorientation of the liquid crystal was sometimes referred to as the linear instability [4,5,8–11]. We do the calculation in a different way with the detailed derivation presented. In the coordinate depicted in Fig. 1, the director is described by

$$\vec{n}=[n_x(z),n_y(z),n_z(z)]. \tag{9}$$

The flow of the liquid crystal produces a torque on the liquid crystal, which depends on the symmetric part of the velocity gradient tensor $\overleftrightarrow{A}$ whose nonzero components are

$$A_{yz}=A_{zy}=\frac{1}{2}\frac{du^{\text{let}}}{dz}=A. \tag{10}$$

There is another viscosity torque due to the rotation of the liquid crystal. It depends on the net rotation velocity, which is given by

$$\vec{N}=\frac{d\vec{n}}{dt}-\vec{\varpi}. \tag{11}$$

$\vec{\varpi}$ is the angular velocity of the liquid crystal when the liquid crystal rotates as a whole. It is related to the antisymmetric part of the velocity gradient tensor and is given by

$$\vec{\varpi}=\tfrac{1}{2}\nabla\times\vec{V}=(-A,0,0). \tag{12}$$

The total viscous torque is given by

$$\vec{\Gamma}_{\text{vis}}=-\gamma_1\vec{n}\times\vec{N}-\gamma_2\vec{n}\times(\overleftrightarrow{A}\cdot\vec{n})=\vec{n}\times(-\gamma_1\vec{N}-\gamma_2\overleftrightarrow{A}\cdot\vec{n}), \tag{13}$$

where γ_1 and γ_2 are the rotational viscosity coefficients. There is an elastic torque $\vec{\Gamma}_{\text{ela}}$ due to the elastic distortion of the liquid crystal, which is given by

$$\vec{\Gamma}_{\text{ela}}=\vec{n}\times\vec{h}, \tag{14}$$

where $\vec{h}$ is the molecular field. The elastic torque is derived from the elastic energy density. In the case we are considering, the director is dependent only on z, and the components of the molecular field are given by

$$h_i=-\frac{\partial f}{\partial n_i}+\sum_j\frac{\partial}{\partial x_j}\frac{\partial f}{\partial(\partial n_i/\partial x_j)}=-\frac{\partial f}{\partial n_i}+\frac{\partial}{\partial z}\frac{\partial f}{\partial(\partial n_i/\partial z)}. \tag{15}$$

At low speeds, the inertial term is much smaller than the viscous and elastic torques and can be neglected. The elastic and viscous torques balance each other,

$$\vec{\Gamma}_{\text{ela}}+\vec{\Gamma}_{\text{vis}}=\vec{n}\times(\vec{h}-\gamma_1\vec{N}-\gamma_2\overleftrightarrow{A}\cdot\vec{n})=0. \tag{16}$$

Equation (16) means that $(\vec{h}-\gamma_1\vec{N}-\gamma_2\overleftrightarrow{A}\cdot\vec{n})$ is parallel to $\vec{n}$, that is,

$$\vec{h}-\gamma_1\vec{N}-\gamma_2\overleftrightarrow{A}\cdot\vec{n}=a(z)\vec{n}, \tag{17}$$

where $a(z)$ is a constant depending on z. Presented in x, y, and z components, the above equation becomes

$$h_x-\gamma_1\frac{\partial n_x}{\partial t}=an_x,$$

$$h_y-\gamma_1\frac{\partial n_y}{\partial t}+\gamma_1An_z-\gamma_2An_z=an_y,$$

$$h_z-\gamma_1\frac{\partial n_z}{\partial t}-\gamma_1An_y-\gamma_2An_y=an_z.$$

Eliminating a in the above equations, we obtain

$$\gamma_1 n_y \frac{\partial n_x}{\partial t} - \gamma_1 n_x \frac{\partial n_y}{\partial t} = n_y h_x - n_x h_y + (\gamma_2 - \gamma_1) A n_x n_z, \tag{18}$$

$$\gamma_1 n_z \frac{\partial n_x}{\partial t} - \gamma_1 n_x \frac{\partial n_z}{\partial t} = n_z h_x - n_x h_z + (\gamma_2 + \gamma_1) A n_x n_y. \tag{19}$$

The liquid crystal director $\vec{n}$ can be expressed as a function of the polar angle θ and the azimuthal angle ϕ,

$$\begin{aligned} n_x &= \sin\theta(z)\cos\phi(z), \\ n_y &= \sin\theta(z)\sin\phi(z), \\ n_z &= \cos\theta(z). \end{aligned} \tag{20}$$

The elastic energy density is

$$f = \tfrac{1}{2}(K_{11}\sin^2\theta + K_{33}\cos^2\theta)\left(\frac{\partial\theta}{\partial z}\right)^2 + \tfrac{1}{2}(K_{22}\sin^2\theta + K_{33}\cos^2\theta)\sin^2\theta\left(\frac{\partial\phi}{\partial z}\right)^2. \tag{21}$$

The molecular field can be calculated by

$$h_i = -\frac{\delta f}{\delta n_i} = -\frac{\delta f}{\delta\theta}\frac{\partial\theta}{\partial n_i} - \frac{\delta f}{\delta\phi}\frac{\partial\phi}{\partial n_i} \quad (i = x,y,z). \tag{22}$$

Using Eqs. (20), (21), and (22), Eqs. (18) and (19) become

$$\begin{aligned} \gamma_1 \frac{\partial\theta}{\partial t} &= (K_{11}\sin^2\theta + K_{33}\cos^2\theta)\frac{\partial^2\theta}{\partial z^2} \\ &\quad + (K_{11} - K_{33})\sin\theta\cos\theta\left(\frac{\partial\theta}{\partial z}\right)^2 \\ &\quad - [2K_{22}\sin^2\theta + K_{33}\cos(2\theta)] \\ &\quad \times \sin\theta\cos\theta\left(\frac{\partial\phi}{\partial z}\right)^2 + (\gamma_2 + \gamma_1)A\sin^2\theta\sin\phi \\ &\quad - (\gamma_2 - \gamma_1)A\cos^2\theta\sin\phi, \end{aligned} \tag{23}$$

$$\begin{aligned} \gamma_1 \sin\theta\frac{\partial\phi}{\partial t} &= (K_{22}\sin^2\theta + K_{33}\cos^2\theta)\sin\theta\frac{\partial^2\phi}{\partial z^2} \\ &\quad + 2[2K_{22}\sin^2\theta + K_{33}\cos(2\theta)]\cos\theta\frac{\partial\theta}{\partial z}\frac{\partial\phi}{\partial z} \\ &\quad - (\gamma_2 - \gamma_1)A\cos\theta\cos\phi. \end{aligned} \tag{24}$$

The boundary conditions are

$$\theta\left(z = \frac{-d}{2}\right) = \theta\left(z = \frac{d}{2}\right) = \frac{\pi}{2},$$

$$\phi\left(z = \frac{-d}{2}\right) = \phi\left(z = \frac{d}{2}\right) = 0.$$

In the steady state, $\partial\theta/\partial t = 0$ and $\partial\phi/\partial t = 0$. Equations (23) and (24) become

$$\begin{aligned} &(K_{11}\sin^2\theta + K_{33}\cos^2\theta)\frac{\partial^2\theta}{\partial z^2} \\ &\quad + (K_{11} - K_{33})\sin\theta\cos\theta\left(\frac{\partial\theta}{\partial z}\right)^2 \\ &\quad - [2K_{22}\sin^2\theta + K_{33}\cos(2\theta)]\sin\theta\cos\theta\left(\frac{\partial\phi}{\partial z}\right)^2 \\ &\quad + (\gamma_2 + \gamma_1)A\sin^2\theta\sin\phi - (\gamma_2 - \gamma_1) \\ &\quad \times A\cos^2\theta\sin\phi = 0, \end{aligned} \tag{25}$$

$$\begin{aligned} &(K_{22}\sin^2\theta + K_{33}\cos^2\theta)\sin\theta\frac{\partial^2\phi}{\partial z^2} \\ &\quad + 2[2K_{22}\sin^2\theta + K_{33}\cos(2\theta)]\cos\theta\frac{\partial\theta}{\partial z}\frac{\partial\phi}{\partial z} \\ &\quad - (\gamma_2 - \gamma_1)A\cos\theta\cos\phi = 0. \end{aligned} \tag{26}$$

At the surface of the plate, if the liquid crystal is anchored along the y direction, the solutions in bulk for the above equations are $\phi = \pi/2$ and $\theta = \theta_0$, given by

$$\begin{aligned} (\gamma_2 + \gamma_1)A\sin^2\theta - (\gamma_2 - \gamma_1)A\cos^2\theta = 0, \\ \cos 2\theta_0 = \frac{\gamma_1}{\gamma_2}. \end{aligned} \tag{27}$$

θ_0 is called the flow alignment angle. As an example, for nematic liquid crystal 5CB, $\gamma_1 = 81\times10^{-3}$ N s/m^2, $\gamma_2 = -85\times10^{-3}$ N s/m^2, $\theta_0 = 81.18°$ [12].

At the surface of the plate, if the liquid crystal is anchored along the x direction, when the flow speed is low, the liquid crystal is in the ground state and the director is uniformly aligned along the x direction; $\theta = \pi/2$ and $\phi = 0$. When the flow speed gradient is sufficiently high, the liquid crystal reorients. There is a critical flow speed gradient. When the flow speed gradient is slightly higher than the critical value, the distortion is small. For small distortion, ϕ is small and θ is close to $\pi/2$. We define $\alpha = \theta - \pi/2$, then α is small. $\sin\phi \simeq \phi$, $\cos\phi \simeq 1$, $\sin\theta = \cos\alpha \simeq 1$, and $\cos\theta = -\sin\alpha = -\alpha$. Keeping the first-order terms, Eqs. (25) and (26) become

$$K_{11}\frac{\partial^2\alpha}{\partial z^2} = -(\gamma_2 + \gamma_1)A\phi, \tag{28}$$

$$K_{22}\frac{\partial^2\phi}{\partial z^2} = -(\gamma_2 - \gamma_1)A\alpha. \tag{29}$$

The boundary conditions are

$$\alpha\left(z = \frac{-d}{2}\right) = \alpha\left(z = \frac{d}{2}\right) = 0, \tag{30}$$

$$\phi\left(z = \frac{-d}{2}\right) = \phi\left(z = \frac{d}{2}\right) = 0. \tag{31}$$

In the ground (undistorted) state, $\alpha(z) = 0$, $\phi(z) = 0$. There is a critical flow speed gradient A_c. When $A < A_c$, the liquid

crystal is in the undistorted state with $\vec{n}=\hat{x}$. When $A \geq A_c$, the liquid crystal is in the distorted state with nonzero n_y and n_z. We will show that this transition is second order and may be called the flow-induced Freedericksz transition because of the similarity with the field-induced Freedericksz transition. As an example, let us consider the case where the velocity has a linear profile,

$$u(z)=\begin{cases} 2V\left(\dfrac{z}{d}+\dfrac{1}{2}\right), & \dfrac{-d}{2}\leq z\leq 0, \\ -2V\left(\dfrac{z}{d}-\dfrac{1}{2}\right), & 0\leq z\leq \dfrac{d}{2}, \end{cases} \tag{32}$$

where V is the flow speed at the middle layer.

$$A=\begin{cases} \dfrac{2V}{d}=A_0, & \dfrac{-d}{2}\leq z<0, \\ -\dfrac{2V}{d}=-A_0, & 0<z\leq \dfrac{d}{2}. \end{cases} \tag{33}$$

Let $\phi=\phi_1(z)$ and $\theta=\theta_1(z)$ in the region $-d/2\leq z\leq 0$, $\phi=\phi_2(z)$ and $\theta=\theta_2(z)$ in the region $0\leq z\leq d/2$. The equations for them are

$$K_{11}\frac{\partial^2\alpha_1}{\partial z^2}=-(\gamma_2+\gamma_1)A_0\phi_1, \tag{34}$$

$$K_{22}\frac{\partial^2\phi_1}{\partial z^2}=-(\gamma_2-\gamma_1)A_0\alpha_1, \tag{35}$$

$$K_{11}\frac{\partial^2\alpha_2}{\partial z^2}=(\gamma_2+\gamma_1)A_0\phi_2, \tag{36}$$

$$K_{22}\frac{\partial^2\phi_2}{\partial z^2}=(\gamma_2-\gamma_1)A_0\alpha_2. \tag{37}$$

The boundary conditions are

$$\begin{gathered} \phi_1\left(z=-\frac{d}{2}\right)=0, \\ \alpha_1\left(z=-\frac{d}{2}\right)=0, \\ \phi_2\left(z=\frac{d}{2}\right)=0, \\ \alpha_2\left(z=\frac{d}{2}\right)=0, \\ \phi_1(z=0)=\phi_2(z=0), \\ \alpha_1(z=0)=\alpha_2(z=0), \\ \frac{\partial\phi_1}{\partial z}(z=0)=\frac{\partial\phi_2}{\partial z}(z=0), \\ \frac{\partial\alpha_1}{\partial z}(z=0)=\frac{\partial\alpha_2}{\partial z}(z=0). \end{gathered} \tag{38}$$

We have the symmetry $\phi_1(-z)=\phi_2(z)$, $\alpha_1(-z)=-\alpha_2(z)$ or $\phi_1(-z)=-\phi_2(z)$, $\alpha_1(-z)=\alpha_2(z)$ (which has the same critical flow speed gradient) [10]. The solution of Eqs. (34) and (35) is

$$\phi_1(z)=B_1e^{qz}+B_2e^{-qz}+B_3\cos(qz)+B_4\sin(qz), \tag{39}$$

$$\alpha_1(z)=\left(\frac{K_{22}(\gamma_2+\gamma_1)}{K_{11}(\gamma_2-\gamma_1)}\right)^{1/2}[B_1e^{qz}+B_2e^{-qz} -B_3\cos(qz)-B_4\sin(qz)], \tag{40}$$

where $q=([(\gamma_2^2-\gamma_{11}^2)/(K_{11}K_{22})]A_0^2)^{1/4}$. Using the boundary conditions given in Eq. (38), we obtain four independent equations for B_1, B_2, B_3, and B_4. In order to have a nonzero solution for them, it requires

$$\tan(qd/2)=\frac{e^{-qd/2}-e^{qd/2}}{e^{-qd/2}+e^{qd/2}}. \tag{41}$$

The smallest value of q is found to be $q_c=4.730/d$. The critical flow speed gradient is

$$A_c=A_{oc}=2.267\,\frac{\pi^2}{d^2}\left[\frac{K_{11}K_{22}}{\gamma_2^2-\gamma_1^2}\right]^{1/2}. \tag{42}$$

The critical speed is

$$V_0=1.133\,\frac{\pi^2}{d}\left[\frac{K_{11}K_{22}}{\gamma_2^2-\gamma_1^2}\right]^{1/2}. \tag{43}$$

If the liquid crystal is 5CB and the cell thickness is 50 μm, we use the following parameters [12]: $K_{11}=6.4\times10^{-12}$ N, $K_{22}=3.0\times10^{-12}$ N, $\gamma_1=81\times10^{-3}$ N s/m^2, $\gamma_2=-85\times10^{-3}$ N s/m^2, then the critical flow speed is $V_0=38.0$ μm/s.

Nematic liquid crystals are anisotropic fluids and usually have four different translational viscosity coefficients. A flow of a nematic liquid crystal causes it to reorient. When the liquid crystal reorients, the translational viscosity force changes, and so does the velocity field. However, when the flow speed gradient is slightly above the critical value, the distortion of the liquid crystal director is small, and the velocity field can be considered approximately the same as in the undistorted state where the flow velocity profile is parabolic (this will be discussed more later),

$$u(z)=4V\left(\frac{1}{4}-\frac{z^2}{d^2}\right), \quad -\frac{d}{2}\leq z\leq\frac{d}{2}. \tag{44}$$

The flow speed gradient is

$$A=\frac{1}{2}\frac{\partial u}{\partial z}=-\frac{V}{d}\left(4\frac{z}{d}\right). \tag{45}$$

The maximum speed gradient is $2V/d$. We define a parameter measuring the flow speed gradient

$$P=\left(\frac{2V}{d}\right)\Big/\left(\frac{2V_0}{d}\right)=\frac{V}{V_0}, \tag{46}$$

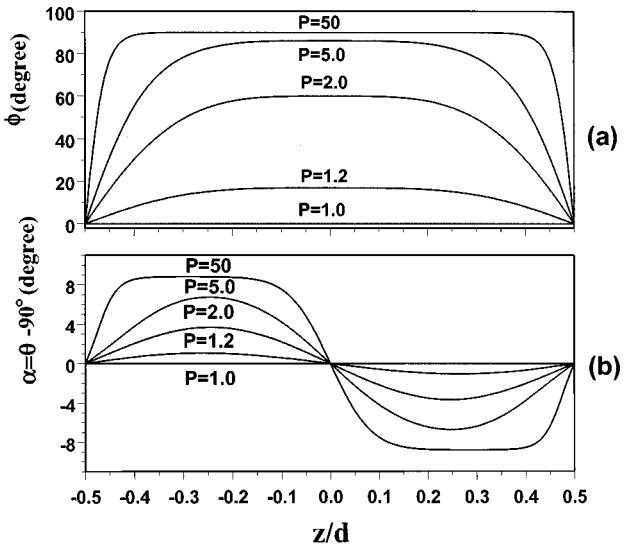

FIG. 2. Polar and azimuthal angles of the liquid crystal director as a function of the coordinate z at various flow speeds.

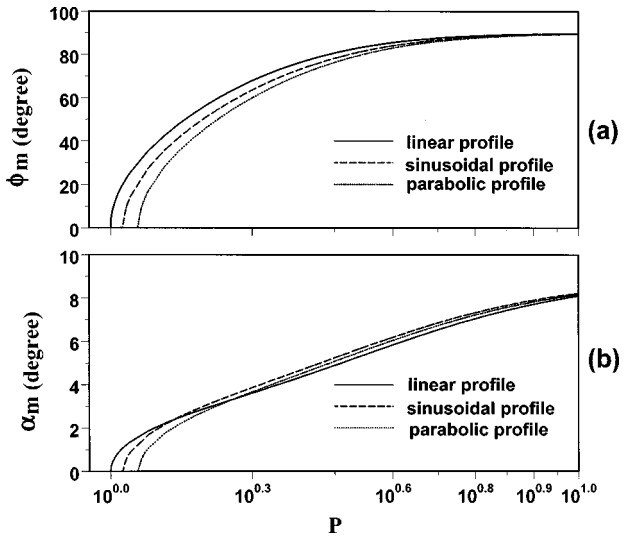

FIG. 3. Maximum deviations as a function of the flow speed.

where V_0 is given by Eq. (43). In this case, the flow speed gradient is not a constant but dependent on z. We numerically solved Eqs. (25) and (26) using the relaxation method. In the calculation, we used Eqs. (23) and (24), and the initial state was the undistorted state with small random fluctuations in ϕ and θ. ϕ and θ changed according to $\phi(t+\Delta t)=\phi(t)+(\partial\phi/\partial t)\Delta t$ and $\theta(t+\Delta t)=\theta(t)+(\partial\theta/\partial t)\Delta t$, respectively. $\partial\phi/\partial t$ and $\partial\theta/\partial t$ were obtained using Eqs. (23) and (24). When the steady state was reached, $\partial\phi/\partial t=0$ and $\partial\theta/\partial t=0$. Under random fluctuations in the initial state, the solution for the steady state sometimes had the symmetry $\phi(-z)=\phi(z)$, $\theta(-z)=-\theta(z)$ and at other times the symmetry $\phi(-z)=-\phi(z)$, $\theta(-z)=\theta(z)$. Here we will only discuss the solution with the symmetry of $\phi(-z)=\phi(z)$, $\theta(-z)=-\theta(z)$. The results of our numerical calculation are shown in Fig. 2. The critical value of P is $P_c=1.15$, which is slightly higher than that in the case of linear velocity profile. When P is above P_c, the liquid crystal director is tilted away from x direction. The azimuthal angle is no longer zero and the maximum deviation ϕ_m occurs at the middle layer of the cell. The polar angle becomes smaller than 90° in the bottom half of the cell and larger than 90° in the top half of the cell; the maximum deviation α_m occurs at the planes $z=\pm d/4$. When the flow speed is very high, the azimuthal angle in the bulk becomes 90°, that is, the liquid crystal director becomes parallel to the flow direction; the polar angle becomes 81.17°, which is the same as the flow alignment angle defined in Eq. (27). The maximum deviations are plotted in Fig. 3 as a function of the flow speed gradient P. The results for linear velocity and sinusoidal [defined as $u(z)=V\sin(\pi z/d)$] profiles are also shown in Fig. 3. From the figure we can see that the velocity profile has a minor effect on the liquid crystal configuration.

EXPERIMENT AND RESULTS

The liquid crystal in our experiment was 5CB doped with black dichroic dye S416 (from Mitsui). The alignment layer used was polyimide (PI2555 from Dupont). In the surface tension measurement, we used both cylindrical capillary tubes and long rectangular cells. The capillary tube had a radius R of 0.467 ± 0.003 mm and was coated with polyimide. For both rubbed and unrubbed polyimide, the rise of the liquid crystal h was almost the same and was 1.10 ± 0.05 cm. The density of 5CB ρ was 1.0065 g/cm^3. Using Eq. (8), the difference of the surface tension between air and polyimide and between liquid crystal and polyimide was $\Delta\gamma=\gamma_{sv}-\gamma_{sl}=hRg\rho/2=2.54\times10^{-2}$ J m^{-2}. The rectangular cell had a thickness $d=49.9\pm0.4$ μm (which is much smaller than the width 5 mm). If the polyimide was rubbed perpendicularly (that is, the rubbing direction is perpendicular to the long side of the rectangular cell), the liquid crystal rise h was 9.6 ± 0.1 cm. If the polyimide was rubbed parallel (that is, the running direction is parallel to the long side of the rectangular cell), the liquid crystal rise h was 9.5 ± 0.1 cm. The surface tension difference, almost independent of the rubbing, was $\Delta\gamma=g\rho hd/2=2.36\times10^{-2}$ J m^{-2}, which was close to the value found using the capillary tube. For future calculation, we use the average value $\Delta\gamma=2.4\times10^{-2}$ J m^{-2}.

In the flow speed measurement, we used rectangular cells which were 10 cm long and 0.5 cm wide. The cell thickness was controlled by glass fiber spacers. The two ends of the cell were open. The liquid crystal was placed at one end of the cell and was capillarily filled into the cell. The liquid crystal flowed from one end of the cell to the other. In the flow speed measurement, the cells were placed on a light viewing box with linearly polarized light. A camcorder was used to record the capillary filling process, then the recorded tape was examined. The time resolution was 30 ms determined by the frame time of the camcorder. We studied the flow speed of the liquid crystal in capillary filling into cells with various thickness. For a 10.1 μm thick cell with parallel rubbed polyimide, the length l of the liquid crystal inside the cell is plotted as a function of time in Fig. 4(a). The flow speed $\bar{u}$ vs time is plotted in Fig. 4(b). As the liquid crystal was filled into the cell, the length l of the liquid crystal increased and therefore the pressure gradient decreased. Thus the flow speed decreased with time. The product of the flow

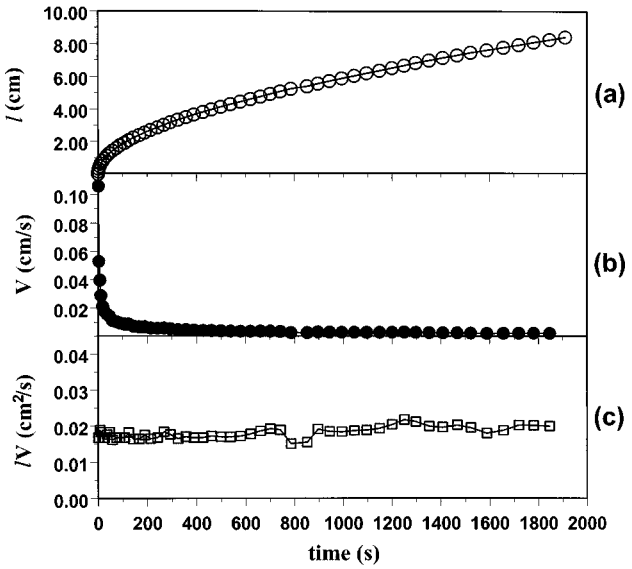

FIG. 4. Flow of the 10 μm cell as a function of time. (a) Liquid crystal length, (b) liquid crystal speed, (c) the product of the liquid crystal length and speed.

speed $\overline{u}$ and the length l of the liquid crystal is plotted as a function of time in Fig. 4(c). It is a constant as predicted by the theory [see Eq. (7)].

The flow speed $\overline{u}$ of the liquid crystal depended on the cell thickness and the filling time. The flow speed vs time for cells with different thicknesses is shown in Fig. 5. The thicker the cell was, the faster the liquid crystal flow, which is consistent with Eq. (7). The flow speed also depended on the angle between the liquid crystal direction and the flow direction. In the cells with parallel rubbed polyimide, the liquid crystal was parallel to the flow direction, the flow was faster, as shown in Fig. 5(b). In the cells with perpendicular rubbed polyimide, the liquid crystal was perpendicular to the flow direction, and the flow was slower, as shown in Fig. 5(a).

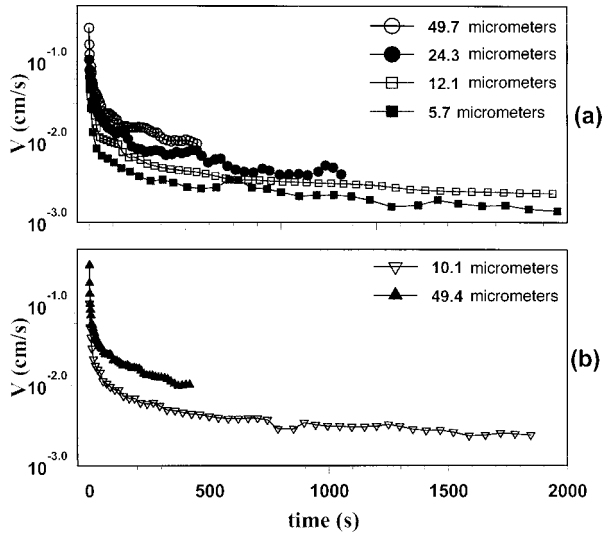

FIG. 5. Flow speeds of cells with different thicknesses as a function of time. (a) Cells with perpendicular rubbed polyimide, (b) cells with parallel rubbed polyimide.

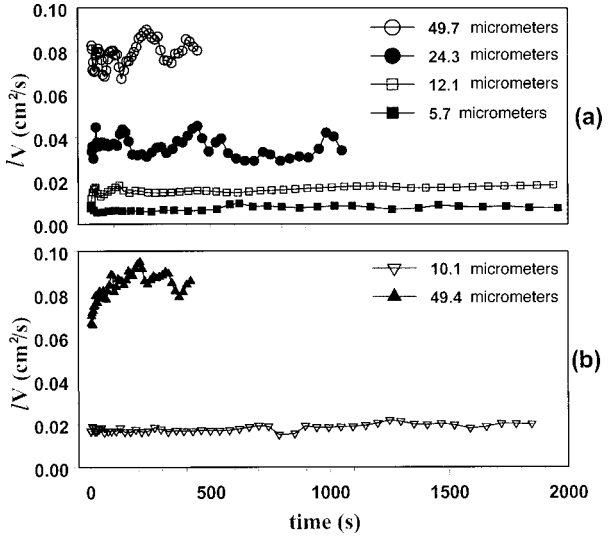

FIG. 6. Product of flow speed and liquid crystal length as a function of time. (a) Cells with perpendicular rubbed polyimide, (b) cells with parallel rubbed polyimide.

The product of the flow speed $\overline{u}$ and the length l of the liquid crystal was dependent on the cell thickness but not on time. $\overline{ul}$ vs time of cells with different thicknesses and alignment layers is plotted in Fig. 6. $\overline{ul}$ was indeed independent of time, except for some fluctuations caused by errors in reading the recorded tape. As given by Eq. (7), $\overline{ul}=[(\gamma_{sv}-\gamma_{sl})/6\eta]d$. $\overline{ul}$ vs the thickness d is a straight line with slope given by $(\gamma_{sv}-\gamma_{sl})/6\eta$. We plot $\overline{ul}$ vs d in Fig. 7. For the cells with parallel rubbed polyimide, the slope was $(1.8\pm0.2)\times10^{-3}$ cm^2/s, the translational viscosity coefficient $\eta=\eta_2=(2.2\pm0.3)\times10^{-2}$ N s/m^2=22$\pm$3 cp. For the cells with perpendicular rubbed polyimide, the slope was $(1.4\pm0.1)\times10^{-3}$ cm^2/s, the translational viscosity coefficient $\eta=\eta_3=(2.9\pm0.2)\times10^{-2}$ N s/m^2=29$\pm$2 cp. Our experimental values are close to the values $\eta_2=22.9$ cp and $\eta_3=37.5$ cp given in the literature [13].

In order to investigate the flow-induced Freedericksz transition, we studied the transmittance of the cells with the perpendicular rubbed polyimide under an optical microscope. The incident light was a white light linearly polarized along

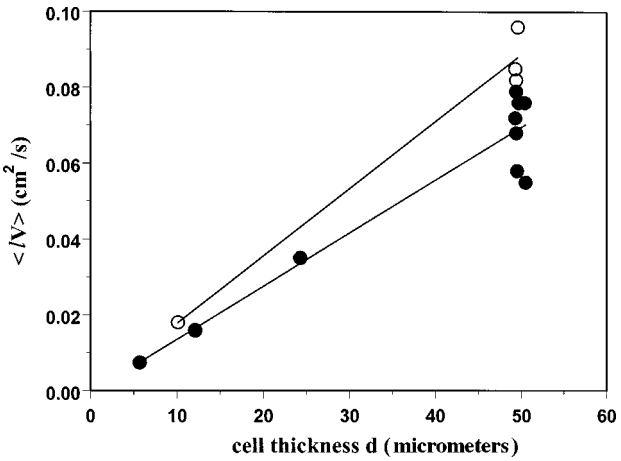

FIG. 7. Average values of the product of flow speed and liquid crystal length as a function of cell thickness.

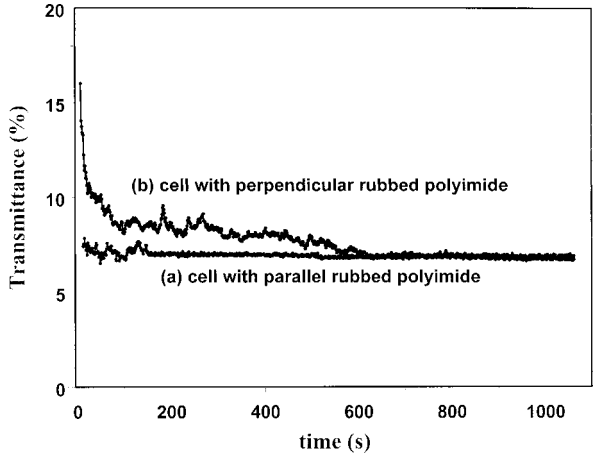

FIG. 8. Transmittance of the 50 μm cell as a function of time. (a) Parallel cell, (b) perpendicular cell.

the rubbing direction of the polyimide. The liquid crystal was doped with 0.4% the dichroic dye. In the experiment, the incident light was focused on a spot about 1 cm away from the entrance end of the cell. The horizontal axis in Figs. 8 and 9 was the filling time started when the liquid crystal was dropped at the entrance end of the cells. We first studied the 50 μm cell with parallel rubbed polyimide and the result is shown in Fig. 8(a). There was no flow-induced Freedericksz transition in this case. In the beginning, there was some intensity fluctuation. Under the optical microscope, flow-induced disclination loops were observed [14]. In the disclination loops, the liquid crystal was not in the same direction as the liquid crystal anchored by the polyimide alignment layers; the absorption of the dye was reduced and therefore the transmittance was increased. As shown in Fig. 8(a), the increase of the transmittance by the disclination loops was small and was not significant. We then studied the 50 μm cell with perpendicular rubbed polyimide. In this cell, we expected to see the flow-induced Freedericksz transition if

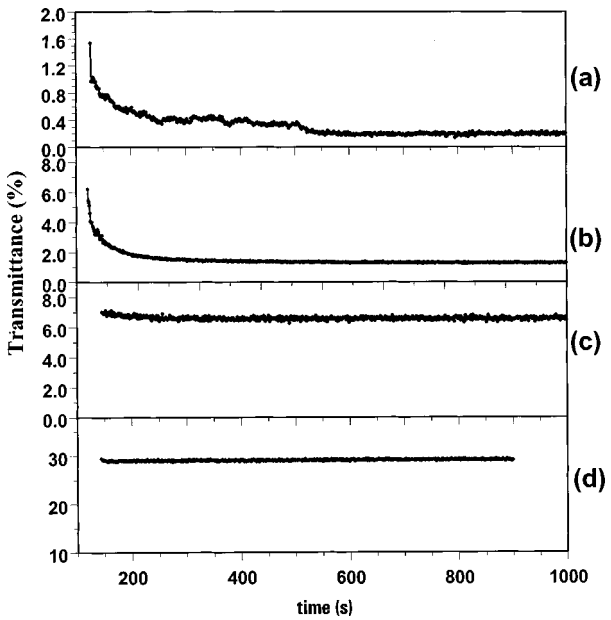

FIG. 9. Transmittance of cells with various thickness as a function of time.

the flow speed was fast enough. When the liquid crystal was in the distorted state induced by the flow, the liquid crystal in the middle of the cell was tilted to the flow direction and the absorption of the dye was reduced, and therefore we expected higher transmittance. In this cell, we indeed observed the flow-induced Freedericksz transition. The transmittance of the cell as a function of time is shown in Fig. 8(b). In the beginning, the transmittance was higher and then decreased with time; after 600 s, the transmittance did not change further. The transition from the distorted state to the undistorted state is a second-order one, as predicted theoretically. Therefore the transmittance decreased continuously to the minimum value of the undistorted state. It was difficult to determine the exact time at which the transmittance decreased to the minimum.

The critical flow speed for the flow-induced Freedericksz transition is inversely proportional to the cell thickness, as indicated in Eq. (43), while the flow speed is proportional to the cell thickness. We expected to observe the flow-induced Freedericksz transition in thick cells but not in thin cells. We measured the transmittance of cells with different thicknesses in the capillary filling. The dye concentration was 2.0%. We made a set of cells with thicknesses 49.7, 24.3, 12.1, and 5.7 μm. The transmittance of the 49.7 μm cell is plotted as a function of time in Fig. 9(a). In this cell, the flow-induced Freedericksz transition was observed. The transmittance in the beginning was high and then decreased gradually to the minimum value at $t=500$ s. For this cell, the theoretically predicted critical value of the speed of the flow front is $\overline{u_c}=\frac{2}{3}\times 1.15V_0\times\frac{50}{49.7}=29.3$ μm/s. As shown in Fig. 5(a), at the beginning, the flow speed was faster than 800 μm/s, which is higher than the critical value; the liquid crystal was in the flow distorted state. As the liquid crystal was filled into the cell, the flow speed decreased; the distortion became smaller and the transmittance decreased. The transmittance decreased to the minimum around $t=500$ s, at which the flow speed was around 95 μm/s. This experimentally observed speed was higher than the predicted value 29.3 μm/s. For the 24.5 μm cell, the result is shown in Fig. 9(b). In the beginning, the transmittance was also high and then decreased gradually with time; after 400 s, the transmittance did not change. As shown in Fig. 5(a), in the beginning, the flow speed was faster than 500 μm/s, and then decreased with time. The flow speed at $t=400$ s was about 60 μm/s, which was very close to the theoretically predicted critical value $\overline{u_c}=\frac{2}{3}\times 1.15\times 37.9\times\frac{50}{24.3}$ μm/s$=59.8$ μm/s. For the 12.1 μm cell, the result is shown in Fig. 9(c). The transmittance was always low and did not change with time. The theoretically predicted critical value of the speed of the flow front is $\overline{u_c}=\frac{2}{3}\times 1.15\times 37.9\times\frac{50}{12.1}$ μm/s$=120$ μm/s. As shown in Fig. 5(a), after 100 s (at which our transmittance measurement was started), the flow speed was less than 100 μm/s, and therefore there was no flow-induced Freedericksz transition. For the 5.7 μm cell, the result is shown in Fig. 9(d). The transmittance was always low and did not change with time. The theoretically predicted critical value of the speed of the flow front is $\overline{u_c}=\frac{2}{3}\times 1.15\times 37.9\times\frac{50}{5.7}$ μm/s$=255$ μm/s. As shown in Fig. 5(a), the flow speed was always less than that value, and therefore there was no flow-induced Freedericksz transition.

We also studied cells with unrubbed polyimide. The liq-

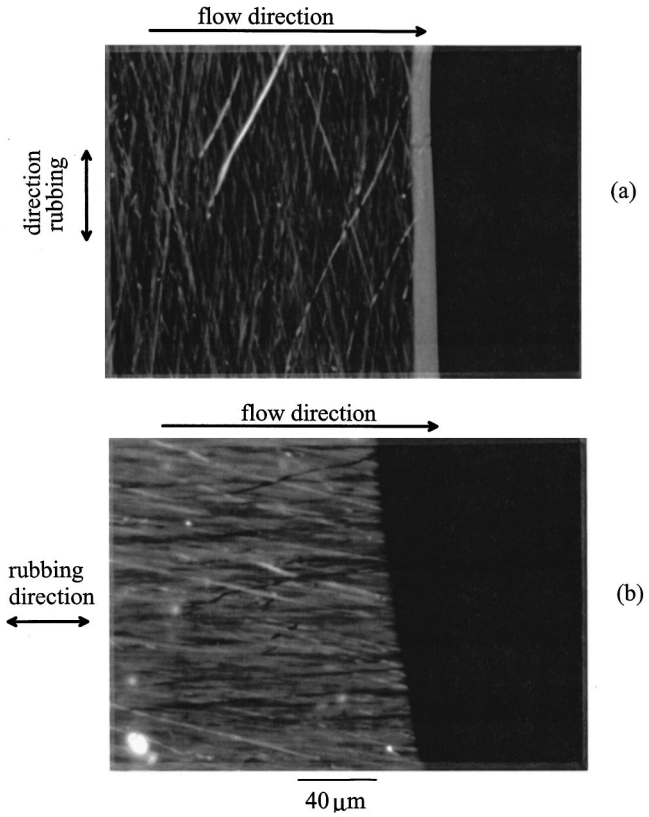

FIG. 10. Microphotograph of the flow front. The fine lines on the left side of the photos are scratches produced in rubbing the polyimide. (a) Cell with perpendicular rubbed polyimide, (b) cell with parallel rubbed polyimide.

uid crystal was doped with the black dichroic dye. When the polarization of the incident light was parallel to the flow direction, the cells were black, indicating the liquid crystal was aligned along the flow direction in the capillary filling.

We examined the liquid crystal flow front in the capillary filling under an optical microscope with crossed polarizers. The flow direction was either parallel or perpendicular to the polarizers. For the cells with parallel rubbed or unrubbed polyimide, the orientation of the liquid crystal was the same, along the flow direction in both the flow front and behind the flow front. For the cells with perpendicular rubbed polyimide, the flow front was bright as shown the microphotograph in Fig. 10(a). We believe the liquid crystal in the flow front had the twisted configuration shown in Fig. 11. In this case, some care should be taken in capillary filling, because the liquid crystal may exert a torque on the molecules of the alignment layer and damage the alignment layer. We did not

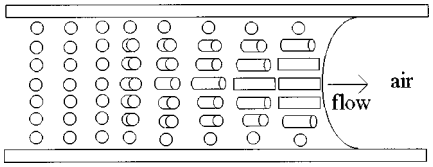

FIG. 11. Liquid crystal director configuration in the flow front in cells with perpendicular rubbed polyimide.

observe the bright flow front in cells with parallel rubbed or unrubbed polyimide. A microphotograph of the flow front of a cell with parallel rubbed polyimide is shown in Fig. 10(b). In cells with perpendicular rubbed polyimide, independent of the cell thickness and the speed of the flow, the bright flow front was always observed. We also made cells with only one open end and perpendicular rubbed polyimide. We observed the bright front when the liquid crystal was filled into the cells in a vacuum chamber. We think that the twisted configuration of the liquid crystal is caused by the perpendicular anchoring of the liquid crystal on the front liquid crystal-air or liquid crystal-vacuum interface.

CONCLUSION

We have theoretically and experimentally studied capillary filling of nematic liquid crystals into cells with various anchoring conditions and thickness. We found that the flow speed of the liquid crystal in the capillary filling was inversely proportional to the cell thickness. In cells with parallel rubbed or unrubbed polyimide, the liquid crystal was oriented parallel to the flow direction in both the flow front and behind the flow front. In cells with perpendicular rubbed polyimide, the orientation of the liquid crystal was dependent on the position in the flow. In the flow front, the liquid crystal was in a twisted configuration with the liquid crystal in the middle of the cell parallel to the flow direction. Far behind the flow front, when the flow speed was low, the liquid crystal at the surface and inside the cell was oriented parallel to the anchoring direction. At high flow speed, the liquid crystal at the surface of the cell was oriented parallel to the anchoring direction, while in the middle of the cell the liquid crystal was aligned parallel to the flow direction. The observed critical flow speeds in cells with different thicknesses agreed with the theoretical predicted ones.

ACKNOWLEDGMENTS

This research was supported in part by ARPA under Contract No. N61331-94-K-0042 and the NSF under ALCOM Grant No. DMR89-2014.

[1] For review of surface anchoring of liquid crystals, see E. Guyon and W. Urbach, in *Nonemissive Electrooptic Displays*, edited by A. R. Kmetz and F. K. von Willisen (Plenum, New York, 1976), p. 121; T. Uchida and H. Seki, in *Liquid Crystals Applications and Uses*, edited by B. Bahadur (World Scientific, Singapore, 1992), Vol. 3, p. 1.

[2] For review of hydrodynamics of nematic liquid crystals, see W. H. de Jeu, *Physical Properties of Liquid Crystal Materials* (Gordon and Breach, New York, 1980), pp. 97–121.

[3] P. G. de Gennes and J. Prost, *The Physics of Liquid Crystals* (Oxford University Press, New York, 1993).

[4] E. Guyon and P. Pieranski, J. Phys. (Paris), Colloq. **C1**, 203 (1975).

[5] P. Manneville and E. Dubois-Violette, J. Phys. (France) **37**, 285 (1976).

[6] For a review of back flow, see S. Chandrasekhar, *Liquid Crys-*

tals (Cambridge University Press, Cambridge, 1992), pp. 162–167.

[7] D. J. Barber and R. Loudon, *An Introduction to the Properties of Condensed Matter* (Cambridge University Press, Cambridge, 1989).

[8] P. Pieranski and E. Guyon, Solid State Commun. **13**, 435 (1973).

[9] P. Pieranski and E. Guyon, Phys. Rev. A **9**, 404 (1974).

[10] I. Janossy, P. Pieranski, and E. Guyon, J. Phys. (France) **37**, 1105 (1976).

[11] P. Manneville and E. Dubois-Violette, J. Phys. (France) **37**, 1115 (1976).

[12] L. M. Blinov and V. G. Chidrinov, *Electrooptical Effects in Liquid Crystal Materials* (Springer-Verlag, New York, 1994), p. xiv.

[13] G. Vertogen and W. H. de Jeu, *Thermotropic Liquid Crystals, Fundamentals* (Springer-Verlag, Berlin, 1988), p. 152.

[14] P. T. Mather, D. S. Pearson, and R. G. Larson, Liq. Cryst. **20**, 527 (1996).